Rock and Soil Mechanics

Volume 42 | Issue 3 Article 6

7-28-2021

Model tests of large-diameter single pile under horizontal cyclic loading in sand

Ji-meng ZHANG
Key Laboratory of Geotechnical and Underground Engineering of Ministry of Education, Tongji University, Shanghai 200092, China

Chen-rong ZHANG
Key Laboratory of Geotechnical and Underground Engineering of Ministry of Education, Tongji University, Shanghai 200092, China, zcrong33@tongji.edu.cn

Kai ZHANG
East China Architectural Design & Research Institute Co., Ltd, Shanghai 200002, China

Custom Citation

ZHANG Ji-meng, ZHANG Chen-rong, ZHANG Kai, . Model tests of large-diameter single pile under horizontal cyclic loading in sand[J]. Rock and Soil Mechanics, 2021, 42(3): 783-789.

Rock and Soil Mechanics 2021 42(3): 783−789 ISSN 1000−7598
https: //doi.org/10.16285/j.rsm.2020.5597 rocksoilmech.researchcommons.org/journal

Model tests of large-diameter single pile under horizontal cyclic loading in sand

ZHANG Ji-meng[1, 2], ZHANG Chen-rong[1, 2], ZHANG Kai[1, 2, 3]

1. Department of Geotechnical Engineering, Tongji University, Shanghai 200092, China
2. Key Laboratory of Geotechnical and Underground Engineering of Ministry of Education, Tongji University, Shanghai 200092, China
3. East China Architectural Design & Research Institute Co., Ltd, Shanghai 200002, China

Abstract: A series of 1*g* model tests was carried out using a motor servo horizontal cyclic loading equipment to study the stiffness and cumulative displacement of the large-diameter single pile in sand under horizontal cyclic loading. The test results indicated that the residual displacement generated by one loading and unloading cycle is about 80% of the peak displacement. As the number of cycles increases, the area of the cyclic loading hysteresis curve gradually decreases, indicating that the behavior of soil around the pile changes from elastoplastic to elastic stage. The secant stiffness of the hysteretic curve increases firstly and then decreases with the increase of the number of cycles, which is caused by the trend that the soil around the pile is gradually dense, and the resistance of the soil around the pile is developing from shallow to deep. The secant stiffness of the hysteretic curve increases firstly and then decreases with the increase of the number of cycles, which is caused by the progressive compaction of the soil around the pile in the shallow layer and the tendency of the resistance of the soil around the pile to transfer from the shallow layer to the deep layer. The cumulative displacement of the pile top decreases to approximately the same extent as the pile diameter increases. However, with the increase of burial depth, the reduction of displacement also gradually decreases, revealing the existence of critical burial depth. An empirical model of cyclic cumulative displacement is proposed by linear fitting in a double logarithmic coordinate system based on the exponential model. It is found that the effect of increasing the pile diameter on the reduction of cyclic cumulative displacement is superior to that of increasing the buried depth.

Keywords: large-diameter single pile foundation; horizontal cyclic loading; 1*g* model test; cumulative displacement

1 Introduction

Large-diameter steel pipe piles are commonly used as the foundation for offshore wind power equipment. During the operation of wind power generation equipment, the foundation of the equipment has cumulative deformation (displacement) due to the long-term horizontal cyclic loading such as wind and wave. When the deformation of the pile shaft exceeds the limit value, the offshore wind turbine located on the upper part of the pile structure will not work normally. Therefore, it is of great significance to study the stiffness and deformation development of pile foundation under horizontal cyclic loading for the design of the large-diameter steel pipe pile foundation of offshore wind power equipment.

Nowadays, many researchers have carried out a series of experimental studies on the stiffness and deformation characteristics of pile foundation under horizontal cyclic loading. Some studies have focused on the validation and improvement of the *p*-*y* curves of pile foundation based on API code. Through tests, Bayton et al.[1] found that the deflection and bending moment of the large-diameter pile calculated using the *p*-*y* curve method based on API code were smaller than the measured values. Zhu et al.[2] carried out the centrifugal model tests on the large-diameter single pile in sand under horizontal cyclic loading. They proposed the cyclic weakening factor related to the cyclic stress ratio, and modified the hyperbolic *p*-*y* curve, finally obtaining the *p*-*y* curve model considering the number of cycles. Chen et al.[3] conducted the horizontal cyclic loading tests on the pile foundation in saturated silt and introduced the coefficient of cyclic effect that could consider the number of cycles to improve the *p*-*y* curve method.

In addition, some studies focus on the influence of the amplitude of cyclic loading, loading path and the relative density of soil on the cumulative displacement of pile top and the stiffness of the soil beside the pile. Li et al.[4] and Wang et al.[5] conducted the centrifugal model tests on the large-diameter single pile under one-way cyclic loading in the dry sand and saturated sand, respectively. The empirical formula in logarithmic form for the cumulative displacement of pile top with the number of cycles was proposed, and the variation characteristics of soil deformation around the pile and the corresponding

Received: 13 May 2020 Revised: 28 December 2020
This work was supported by the National Nature Science Foundation of China(51779175).
First author: ZHANG Ji-meng, male, born in 1996, Master candidate, mainly engaged in the research of pile foundation engineering. E-mail: 1832582@tongji.edu.cn
Corresponding author: ZHANG Chen-rong, female, born in 1982, Associate researcher, mainly engaged in the research and teaching of pile foundation engineering. E-mail: zcrong33@tongji.edu.cn

excess pore pressure with the amplitude of cyclic loading were discussed. Ding et al.[6] performed the centrifugal model tests on the large-diameter single pile and pile group in clay under horizontal cyclic loading, and discussed the variable characteristics of the ratio of maximum displacement to residual displacement of pile top and the ratio of the maximum bending strain to residual bending strain of pile shaft with the number of cyclic loading. Leblanc et al.[7] proposed the loading path parameters used for describing the characteristics of cyclic loading. Based on the centrifugal model tests on two kinds of sands with different relative densities under one-way and bidirectional cyclic loading, they the exponential empirical formula for the variation of the cumulative rotation angle of single pile top subjected to horizontal cyclic loading with the number of cyclic loading was presented. Arshad and Kelly[8] and Richards et al.[9] carried out the comparative model tests under one-way and bidirectional cyclic loading, and both reached similar conclusions that under the same amplitude of cyclic loading the cumulative displacement caused by asymmetric bidirectional cyclic loading was greater than that caused by one-way cyclic loading. For asymmetric bidirectional cyclic loading, the model tests conducted by Zhang et al.[10] revealed that under a certain number of cyclic loading, the cumulative displacement of pile top increased first and then decreased as the minimum value of loading decreased. Bayton et al.[11] carried out the centrifugal model tests under variable amplitude cyclic loading and verified the feasibility and effectiveness of cyclic degradation model[12] used for analyzing cyclic loading tests.

Although there are many studies on the stiffness and deformation characteristics of pile foundation under horizontal cyclic loading, the existing model tests, and the corresponding prediction models for cyclic cumulative displacement mainly focus on different cyclic loading paths, without considering the effect of pile diameter and buried depth on the cyclic characteristics of large-diameter single piles. To this end, a series of 1*g* model tests on the large-diameter single piles with different diameters and buried depths under the horizontal static loading and cyclic loading was carried out in this study. The static loading and unloading curves, cyclic loading hysteresis loop, and the response of the cumulative displacement of pile top are analyzed, and the effect of diameter and buried depth on the cumulative displacement of pile top is discussed.

2 Testing program and apparatus

2.1 Loading system

The static load testing was completed by loading and unloading the counterweight step by step. The horizontal cyclic loading was realized by using the servo motor. The cyclic loading with controlled force was realized by inputting the time-history curve of cyclic loading. The range of cyclic loading was ± 1 kN with an accuracy of ± 5 N, and the loading frequency was 0.1 Hz. The loading system is shown in Fig. 1. The dimension of the model box used in the test was 50 cm×50 cm×50 cm. The displacements of the pile shaft at 3 cm below the pile top and 1 cm above the ground surface were measured by voltage displacement meter, respectively. The loading of pile top was measured by force sensor.

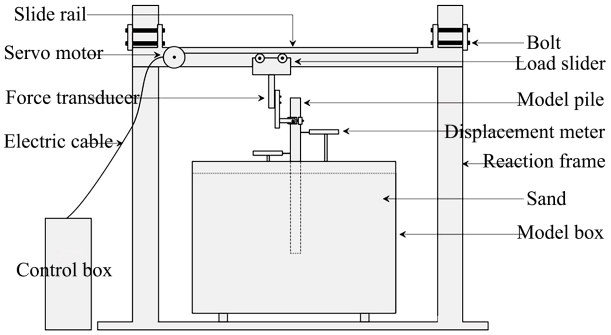

(a) Design drawing of cyclic loading test device

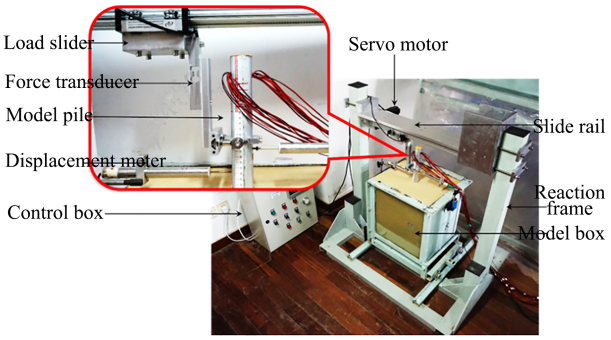

(b) Physical drawing of cyclic loading test device

Fig. 1 Test device

2.2 Preparation of model pile and subsoil

The model pile is made of aluminum alloy pipe. The density of aluminum alloy is 2 700 kg/m^3, the elastic modulus was 68.9 GPa, and the Poisson's ratio is 0.3. The pile top fixture is designed to realize the connection between the actuating device and the pile shaft, as shown in Fig. 2; where L is the height from the loading point to the ground surface; H is the buried depth of the pile; d is the outer diameter of the pile, and δ is the thickness of the pile shaft, with the size of 2 mm.

Japanese Fengpu Sand was used in the test and the grading curve is shown in Fig. 3. For this type of sand, the average particle size is d_{50} = 0.16 mm, the uniformity coefficient C_u = 1.6, the specific weight G_s = 2.64, the maximum void ratio e_{max} = 0.916, and the minimum void ratio e_{min} = 0.609. To simulate the packing characteristics

of sand in the natural state, the pluviation method was adopted to prepare the samples. For the prepared soil sample, the relative density was D_r = 55.3%, and the dry weight was 14.54 kN/m^3. When the thickness of the soil sample in the model box reached the height of the pile bottom, the model pile was placed and fixed, and then the pluviation method was used to make the soil sample thickness meet the requirements.

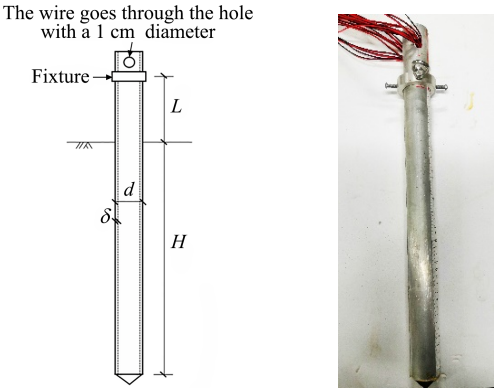

(a) Design drawing (b) Physical picture

Fig. 2 Schematic diagram of model pile

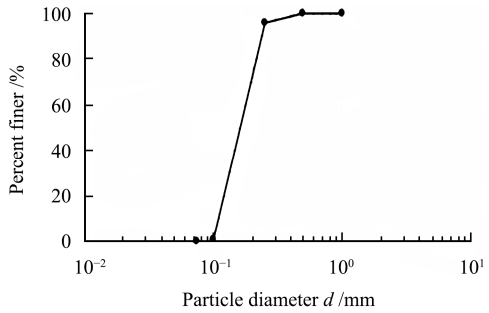

Fig. 3 Grain size distribution curve of soil sample

2.3 Testing program

The piles with four different diameters and four buried depths were selected to carry out static and cyclic loading tests. The similarity ratio of the model pile was 1:100. For the corresponding real pile, the outer diameter was 2−4 m, and the buried depth was 20−35 m. The details of each test model, including pile diameter d, buried depth H, loading height L, ultimate bearing capacity of single pile F_u, cyclic loading amplitude F_c, normalized cyclic loading amplitude ζ_b and the numbers of cyclic loading, are listed in Table 1. The normalized cyclic loading amplitude $\zeta_b = F_c/F_u$ represents the relative magnitude of cyclic loading amplitude and the single pile ultimate bearing capacity, where F_u was obtained from the static load testing in Section 3.1. The cyclic loading adopted sinusoidal unidirectional cyclic loading, and Fig. 4 shows the time−history curve of cyclic loading.

Table 1 Horizontal ultimate bearing capacity of single pile and cyclic loading amplitude

No.	d /cm	H /cm	L /cm	F_u /N	F_c /N	$\zeta_b = F_c/F_u$	Number of cycles
E1	2.0	30	10	17.0	10	0.59	6 000
E2	2.5	30	10	21.0	10	0.48	6 000
E3	3.0	30	10	23.5	10	0.43	6 000
E4	4.0	20	10	15.0	10	0.67	6 000
E5	4.0	25	10	22.5	10	0.44	6 000
E6	4.0	30	10	26.0	10	0.38	6 000
E7	4.0	35	10	38.0	10	0.26	6 000

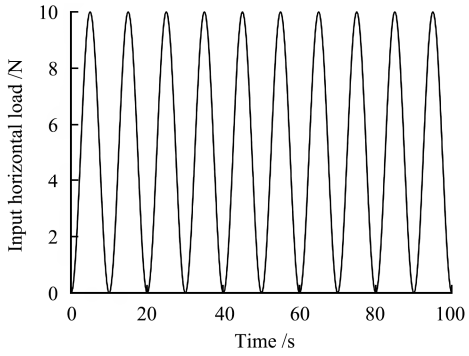

Fig. 4 Time history curve of cyclic loading (the first 100 s)

3 Analysis of test results

3.1 Static load testing

Figure 5 shows the curves of horizontal load and rotation angle at pile top under the static loading and unloading for one time. It can be seen from the figure that for the one-time loading and unloading curve, the initial loading stiffness increases with the increase of pile diameter and buried depth, while the initial unloading stiffness was less affected by pile diameter and buried depth, and the corresponding values in each group were approximately equal. The load corresponding to the rotation angle of 0.5° at pile top was taken as the ultimate bearing capacity of horizontally loaded pile F_u[13], as listed in Table 1.

The maximum load of loading section and the maximum displacement of loading point in each group of static load testing were used to normalize the load−displacement curves under the static loading and unloading for one time, as shown in Fig. 6. As observed in the figure, the normalized loading and unloading curves of load−displacement curves for each group of static load testing were close to the same curve, and the cumulative displacement produced by one-time loading and unloading was about 80% of the peak displacement in the loading process. Under the given loading height and mechanical properties of sand, the buried depth, pile diameter and the magnitude of load under horizontal loading have little influence on the shape of the normalized one-time loading and unloading curve. In Fig. 6, u represents the displacement of loading point for each group of static load testing;

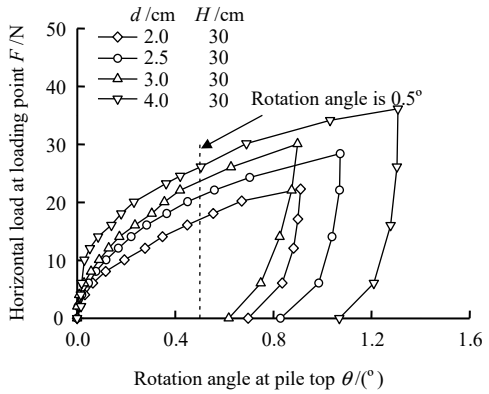

(a) Pile diameter

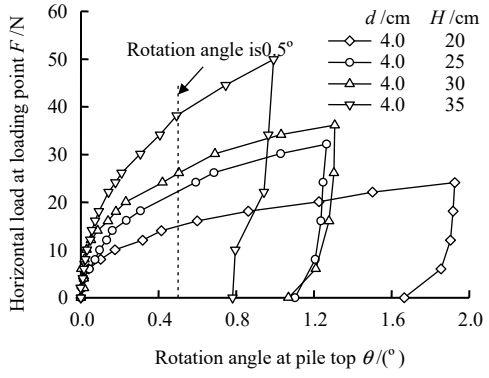

(b) Buried depth

Fig. 5 Load−rotation angle curves at pile top

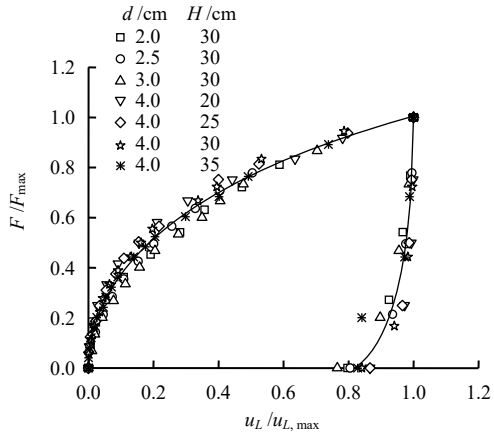

Fig. 6 Normalized load−displacement curves

F and F_{max} are the load and the maximum load at the loading point for each group of static load testing.

3.2 Hysteresis curve of cyclic loading

Figure 7 illustrates the load−displacement hysteretic curves corresponding to the 1st, 10th, 100th, 1 000th, 3 000th and 5 000th cyclic loading in seven groups of cyclic loading tests. With the increase of the number of cycles, the whole hysteresis loop gradually shifts to the right and produced cumulative deformation (displacement) under one-way cyclic loading. The area of hysteresis loop reduces gradually, indicating that the soil behaviors around the pile changes gradually from elastic-plastic to elastic.

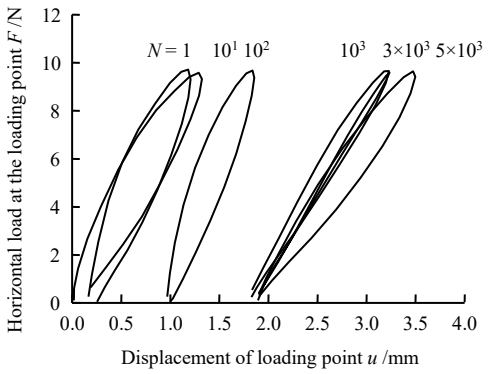

(a) d = 2.0 cm，H = 30 cm

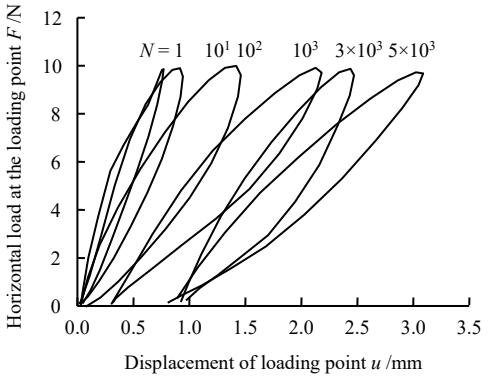

(b) d = 2.5 cm，H = 30 cm

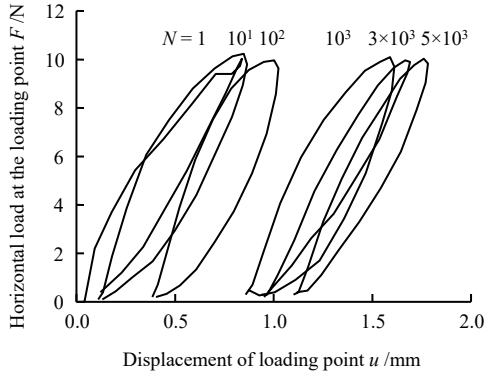

(c) d = 3.0 cm，H = 30 cm

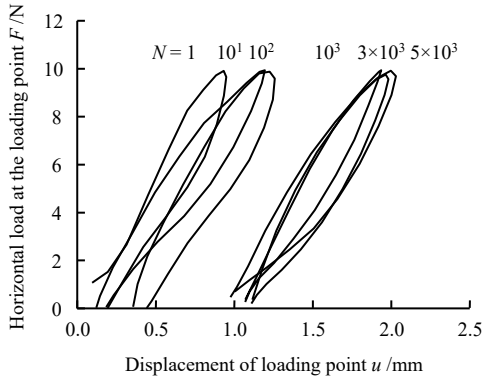

(d) d = 4.0 cm，H = 20 cm

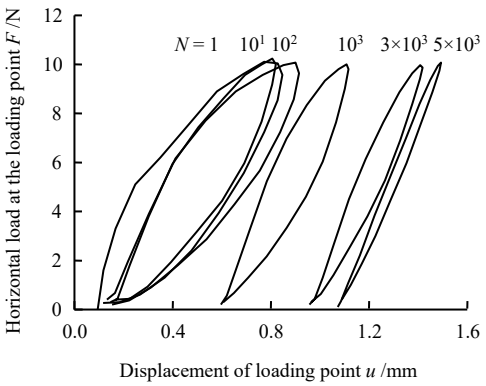

(e) d = 4.0 cm，H = 25 cm

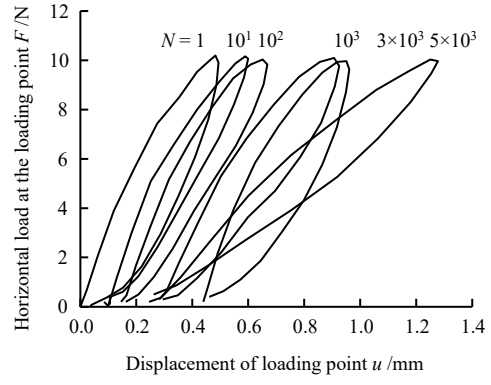

(f) d = 4.0 cm，H = 30 cm

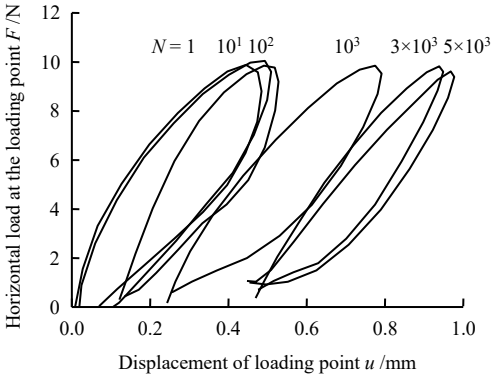

(g) d = 4.0 cm，H = 35 cm

Fig. 7 Load−displacement curves at loading point

Figure 8 shows the relationships between the number of cycles and the global secant stiffness of the hysteresis loop, corresponding to the hysteretic curves under six different cycles in Fig. 7, and the curves normalized by the secant stiffness of the hysteresis loop under the first cyclic loading. Due to the dilatancy of sand, the stiffness of the sand beside the pile changes sharply, and the data are relatively discrete. However, from Fig. 8(b), it can still be seen that the secant stiffness of the hysteresis loop under the 1st, 10th, and 100th cyclic loading had an increasing tendency, while the secant stiffness drops after 100th cyclic loading. This phenomenon might be explained that at the initial stage, the relative density of the shallow sand around the pile gradually rises (becomes denser) with the increase of cyclic loading. However, with the increase of the number of cycles and the cumulative deformation of the pile shaft, the resistance of the soil beside the pile gradually transfers to the deep soil. The relative density of the soil in the deep layer declines under cyclic loading, resulting in a reduction in the overall stiffness of the hysteresis loop. The two sets of data that were obviously inconsistent with the overall regularity might be related to the deviation of output load of servo loading and the inconsistency of sand preparation.

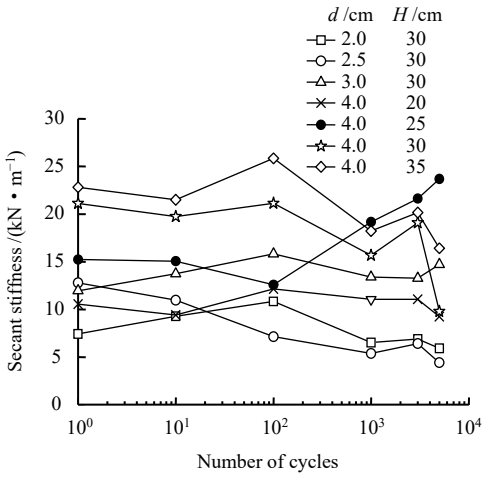

(a) Unnormalized results

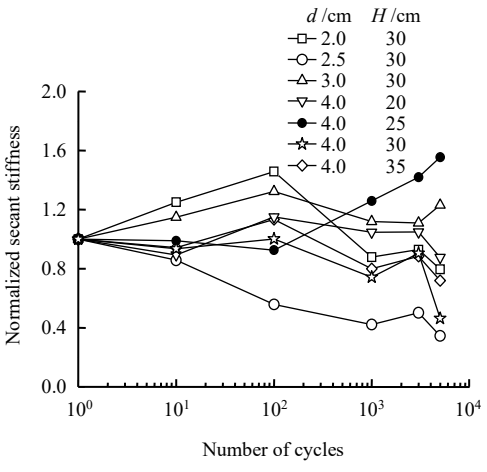

(b) Normalized results

Fig. 8 Relationships between secant stiffness and number of cycles

3.3 Peak horizontal displacement of cyclic loading

The variation of the cumulative peak horizontal displacement of the loading point with the number of cycles is shown in Fig. 9. As seen from Fig. 9, in the first 1 000 cyclic loading, the cumulative deformation grows rapidly with the number of cyclic loading, and after that, the growth rate of cumulative deformation decreases. With

the decrease of pile diameter and buried depth, the cumulative displacement at pile top increases. Within the range of the pile diameter in this work, the cumulative horizontal displacement at pile top caused by the constant amplitude increase of pile diameter also decreases by approximately constant amplitude. However, with the increase of the buried depth of single pile, the decreasing degree of cumulative deformation reduces, indicating that there exists a critical buried depth and the corresponding horizontal cumulative displacement at the top of single pile tended to a certain stable value.

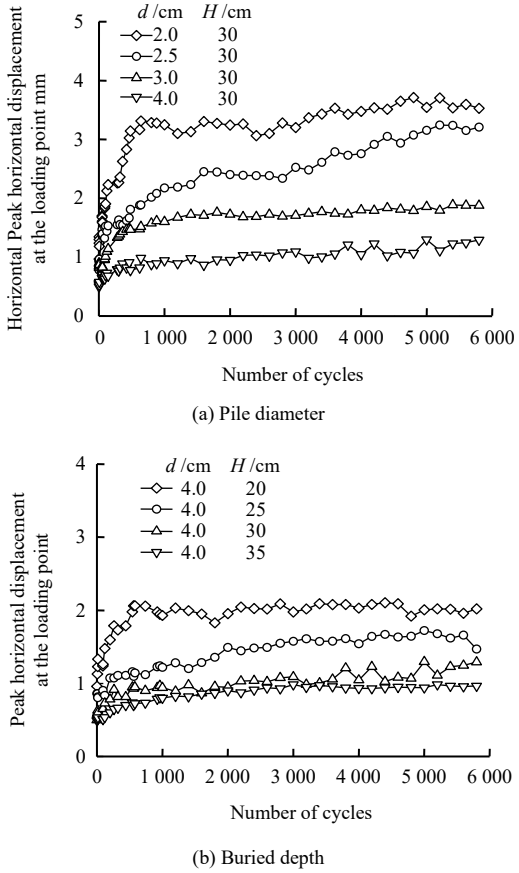

Fig. 9 Relationships between the peak horizontal displacement at pile top and the number of cycles

4 Model of cumulative cyclic displacement at pile top

Little et al.[14] believe that the relationship between cumulative displacement at pile top and the number of cyclic loading for the horizontally loaded pile in sand can be approximately fitted by using exponential function, as shown below:

$$\frac{u_N}{u_1} = N^t \tag{1}$$

where u_1 and u_N are the first horizontal displacement at pile top and the cumulative displacement after N^{th} cyclic loading, respectively; t is an empirical parameter related to the number of cycles. As shown in Fig. 10, the cumulative displacement at pile top under cyclic loading is linearly fitted to the number of cycles in the double logarithmic coordinate system, and the corresponding slope is the empirical parameter t, $t = 0.13$.

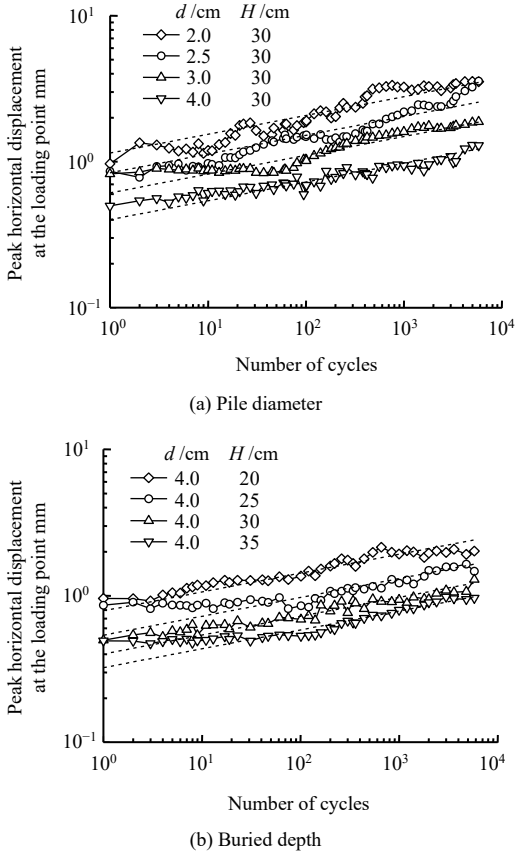

Fig. 10 Comparison of fitting results and experimental results

The relationship between the horizontal displacement at pile top u_1, under the first cyclic loading obtained by linear fitting in Fig. 10 and the amplitude of normalized cyclic loading ζ_b, is shown in Fig. 11. It can be seen that the horizontal displacement at pile top subjected to the first cyclic loading rises with the increase of the amplitude of normalized cyclic loading, and the growth magnitude, i.e., slope, is related to the changes in pile

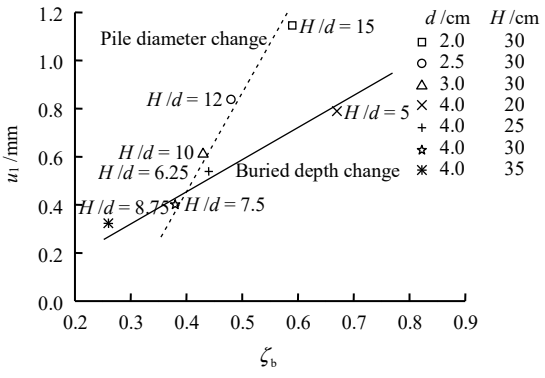

Fig. 11 Relationship between u_1 and ζ_b

https://rocksoilmech.researchcommons.org/journal/vol42/iss3/6
DOI: 10.16285/j.rsm.2020.5597

diameter and buried depth. The slope of the fitting line corresponding to the change of pile top is obviously steeper than the change of buried depth. In combination with Eq. (1), it can be concluded that in practical engineering, the effect of increasing pile diameter on controlling horizontal cumulative displacement at pile top is obviously better than that of increasing pile length.

5 Conclusion

(1) The maximum load and the maximum deformation at pile top are used to normalize the one-time loading and unloading curve. For the loading conditions in this work, the residual deformation of the horizontally loaded pile is about 80% of the maximum displacement. The shape of the normalized load−displacement curve is consistent, and has no obvious correlation with pile diameter, buried depth and the magnitude of load.

(2) The area of cyclic loading hysteresis loop decreases with the increase of the number of cyclic loading, which indicates that the soil behaviors around the pile changes gradually from elastic-plastic to elastic.

(3) The secant stiffness of the hysteretic curve increases gradually in the early stage and then has a decreasing trend. The possible reason is that the initial cyclic loading results in the shallow sand around the pile gradually to compact, while with the increase of the number of cycles, the resistance of soil around the pile transfers from the shallow layer to the deep layer, causing the relative density of deep soil decrease.

(4) Within the range of the pile diameter in this work, the cumulative horizontal displacement at pile top decreases by approximately constant amplitude, with the constant amplitude increase of pile diameter. With the increase of the buried depth of single pile, the decreasing degree of cumulative deformation at pile top decreases accordingly, which indicates that there exists a critical buried depth, and the corresponding horizontal cumulative displacement at the top of single pile tends to a certain stable value.

(5) The exponential model can reasonably reflect the increase of the cumulative displacement at pile top under cyclic loading with the number of cycles.

(6) The analysis of the empirical model demonstrates that in practical engineering, the effect of increasing pile diameter on controlling horizontal cumulative displacement at pile top is obviously superior to that of increasing pile length.

References

[1] BAYTON M S M, BLACK J A. Evaluating the *p–y* curve method of analysis for large-diameter monopiles using Centrifuge Modelling[C]//Geo-Chicago 2016. Chicago: American Society of Civil Engineers, 2016: 418−428.

[2] ZHU Bin, ZHU Rui-yan, LUO Jun, et al. Model tests on characteristics of ocean and offshore elevated piles with large lateral deflection[J]. Chinese Journal of Geotechnical Engineering, 2010, 32(4): 521−530.

[3] CHEN Ren-peng, GU Ming, KONG Ling-gang, et al. Large-scale model tests on high-rise platform pile groups under cyclic lateral loads[J]. Chinese Journal of Geotechnical Engineering, 2012, 34(11): 1990−1996.

[4] LI Z, HAIGH S K, BOLTON M D. Centrifuge modelling of mono-pile under cyclic lateral loads[J]. Physical Modelling in Geotechnics, 2010, 2: 965−970.

[5] WANG Fu-qiang, RONG Bing, ZHANG Ga, et al. Centrifugal model test of pile foundation for wind power unit under cyclic lateral loading[J]. Rock and Soil Mechanics, 2011, 32(7): 1926−1930.

[6] DING Chu, YU Wen-rui, SHI Jiang-wei, et al. Centrifuge studies of pile deformation mechanisms due to lateral cyclic loading[J]. Rock and Soil Mechanics, 2020, 41(8): 2659−2664, 2711.

[7] LEBLANC C, HOULSBY G Y, BYRNE B W. Response of stiff piles in sand to long-term cyclic lateral loading[J]. Geotechnique, 2010, 60(2): 79−90.

[8] ARSHAD M, O'KELLY B C. Model studies on monopile behavior under long-term repeated lateral loading[J]. International Journal of Geomechanics, 2016, 17(1): 04016040.

[9] RICHARDS I A, BYRNE B W, HOULSBY G T. Monopile rotation under complex cyclic lateral loading in sand[J]. Géotechnique, 2019: 1−15.

[10] ZHANG Xun, HUANG Mao-song, HU Zhi-ping. Model tests on cumulative deformation characteristics of a single pile subjected to lateral cyclic loading in sand[J]. Rock and Soil Mechanics, 2019, 40(3): 933−941.

[11] BAYTON M S M, BLACK J A, KLINKVORT R T. Centrifuge modelling of long term cyclic lateral loading on monopiles[C]//Physical Modelling in Geotechnics–ICPMG 2018, [S. l.]: [s. n.], 2018.

[12] ANDERSON K H. Bearing capacity under cyclic loading-offshore, along the coast, and on land[J]. Canadian Geotechnical Journal, 2009, 46(5): 513−535.

[13] KUO Y S, ACHMUS M, ABDEL-RAHMAN K. Minimum embedded length of cyclic horizontally loaded monopoles[J]. Journal of Geotechnical and Geoenvironmental Engineering, 2012, 138(3): 357−363.

[14] LITTLE R L, BRIAUD J L. Full scale cyclic lateral load tests on six single piles in sand[R]. [S. l.]: [s. n.], 1988.